View metadata, citation and similar papers at core.ac.uk

brought to you by CORE

provided by CURVE/open

Pre-bent shape design of full free-form curved beams using isogeometric method and semi-analytical sensitivity analysis

Hosseini, S. F., Moetakef-Imani, B., Hadidi-Moud, S. & Hassani, B.

Author post-print (accepted) deposited by Coventry University's Repository

Original citation & hyperlink:
Hosseini, SF, Moetakef-Imani, B, Hadidi-Moud, S & Hassani, B 2018, 'Pre-bent shape design of full free-form curved beams using isogeometric method and semi-analytical sensitivity analysis', Structural and Multidisciplinary Optimization, vol. 58, no. 6, pp. 2621–2633.
https://dx.doi.org/10.1007/s00158-018-2041-0

DOI 10.1007/s00158-018-2041-0
ISSN 1615-147X
ESSN 1615-1488
Publisher: Springer

The final publication is available at Springer via http://dx.doi.org/10.1007/s00158-018-2041-0

Copyright © and Moral Rights are retained by the author(s) and/ or other copyright owners. A copy can be downloaded for personal non-commercial research or study, without prior permission or charge. This item cannot be reproduced or quoted extensively from without first obtaining permission in writing from the copyright holder(s). The content must not be changed in any way or sold commercially in any format or medium without the formal permission of the copyright holders.

This document is the author's post-print version, incorporating any revisions agreed during the peer-review process. Some differences between the published version and this version may remain and you are advised to consult the published version if you wish to cite from it.

Pre-bent Shape Design of Full Free-Form Curved Beams Using Isogeometric Method and Semi-Analytical Sensitivity Analysis

Seyed Farhad Hosseini [a*], Behnam Moetakef-Imani [b,]

Saeid Hadidi-Moud [c], Behrooz Hassani [b]

[a]*Sun-Air Research Institute, Ferdowsi University of Mashhad, Mashhad, Iran*

[b]*Department of Mechanical Engineering, Ferdowsi University of Mashhad, Mashhad, Iran*

[c]*Research Institute for Future Transport and Cities (FTC), Coventry University, United Kingdom*

Abstract

In this paper, isogeometric analysis (IGA) is employed to solve the problem of a curved beam with free-form geometry, arbitrary loading, and variable flexural/axial rigidity. The main objective of the study is to develop a unified approach for full free-from curved beam problems that can be integrated with a newly developed semi-analytical sensitivity analysis to solve pre-bent shape design problems. The required set of B-spline control points are calculated using an interpolation technique based on chord-length parameterization. The one-to-one correspondence is considered for parameters of the geometry, loading, and rigidity which is proven to have extreme importance. An IGA curved beam element is suggested based on the Euler-Bernoulli beam theory for the general curvilinear coordinate. The validity and effectiveness of the proposed formulation is confirmed by application to a variety of examples. Moreover, three shape optimization examples are taken into consideration. In the first two examples, the pre-bent shapes of spiral and Tschinhausen curved beams with free-form geometry under distributed loading are obtained. In the third example, the pre-bending problem of wind turbine blades is addressed as an industrial example.

Keywords: Isogeometric analysis; Free-form curved beams; Semi-analytical sensitivity analysis; Pre-bending, Parameterization

1. Introduction

Shape optimization (design) deals with finding the best geometric shape satisfying linear/nonlinear constraints of the domain. Three general steps are included in a shape optimization problem: design tool with geometric design variables, structural analysis tool, and optimization tool. FEM and BEM are usually implemented in the design process as the structural analysis tool [1-3]. However, these methods have experienced limitations such as mesh distortion, frequent remeshing, and element locking [3]. Moreover, another disadvantage of FE-based models is their very large design space which leads to rough-irregular solutions. Therefore a post-optimization filtering step is always necessary. Therefore,

tendency toward finding more efficient algorithms has been increased. Meshless methods and IGA are in the spotlight for this purpose. IGA has emerged as an efficient tool since it integrates the first two mentioned steps of the shape optimization problem, i.e. design tool and structural analysis tool. With IGA, the problem with remeshing no longer exists.

The concept of isogeometric analysis (IGA) which has been recently introduced by Hughes et al. [4]can be regarded as an improvement to the well-stablished finite element method (FEM). The meshed geometry required in FEM approximates the perfect geometry which can reduce the accuracy of expected results. IGA takes steps to resolve the shortcoming by employing shape functions based on B-spline, NURBS and T-splines theories. IGA's shape functions not only represent the CAD geometry, but also are considered as a basis for the numerical approximation of the solution space. In other words, IGA allows the integration of the 3D model generated in commercial CAD systems into finite element analysis concepts without extra computational meshes. The developed approach was successfully applied to a wide range of physical problems such as solid mechanics [5-7], fluid mechanics [8, 9], heat transfer [10], and Eigen value problems [11-12]. Moreover, isogeometric analysis was profitably implemented in shape [13, 14], rigidity [15, 16], and topological [17, 18] optimization of various structures.

Despite the recent progress of IGA in shell structures, isogeometric analysis of curved beams demands more improvement efforts. Recent researches in the field focused on the static [19-21], free vibration [22-25], buckling [26, 27], and optimization [28, 29] analyses of curved beams. Thus far, there is no comprehensive model for optimizing the shape of free-form beams under arbitrary distributed loading/rigidity. A schematic model of the aforementioned problem is depicted in Fig. (1). The equivalent beam representing a pre-bent wind turbine blade is an example of such a complex structure and loading.

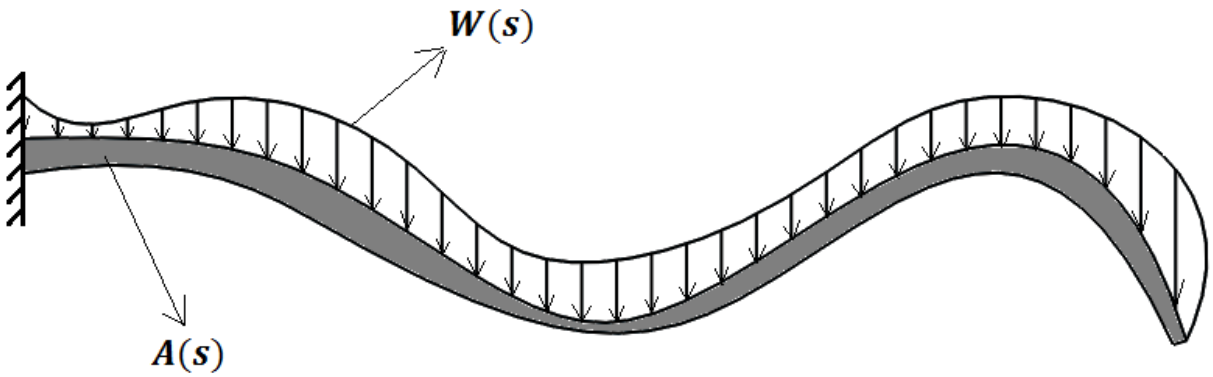

Figure 1 - A beam with free-form curve, loading and cross section

In the study presented by Nagy et al. [29], sizing and shape optimization was performed for maximum fundamental natural frequency. Since their work was devoted to the natural frequency calculations, there was no consideration for loads. Moreover, a method is needed to express the geometry, load and rigidity with a single spline parameter to be applicable in optimization purposes. Based on the order of complexity of a problem, different B-splines may be used to interpolate the shape, the flexural/axial rigidity, and/or the distributed loading. The relationship between aforementioned B-splines' parameterization plays a vital role in the accuracy of solutions which will be categorized as the "analysis

aware modeling". The term "analysis aware modeling" introduced by Cohen et al. [30], emphasizes that the model parameters and properties should be selected so as to facilitate the isogeometric analysis.

It should be noted that an arbitrary distributed set of points representing the curve's shape, rigidity or load can be fitted using B-spline interpolation techniques [31-32]. The interpolated B-spline can be directly used in the framework of isogeometric analysis for all-purpose optimization problems. Since the B-spline control points are regarded as control variables, optimization with IGA is less time consuming and more accurate compared to the conventional FEM optimization. A unified IGA curved beam element is the outcome of the present research which is also extended into pre-bent shape design problems. It should be pointed out that in a pre-bent shape design problem, the deformed configuration of a beam is known and the initial and un-loaded configuration is sought using optimization techniques. A gradient-based method with semi-analytical sensitivity analysis is employed as the optimizer in this paper. An interesting relevant paper was presented by Choi et al. [33] where design sensitivity analysis (DSA) was employed to solve the isogeometric large deformation analysis of curved beams, but in their work, the stiffness and loading were constants.

Both discrete and analytical DSA methods involve the analytical differentiation of discretized geometry equation with respect to design variables. Since finite element and isogeometric analyses stiffness matrices are constructed using numerical integration, the explicit expression of matrices in terms of design variables may not be available and these discrete differentiations may not be achieved easily for general cases. Therefore, a semi-analytical sensitivity analysis is employed in the current research [33].

Henceforth, the article is organized as follows: In Section 2 a brief introduction into B-spline functions is presented and the interpolation method is introduced. Isogeometric analysis formulation of free-form beams under arbitrary distributed loads is presented in Section 3. In this section, the effect of parameterization on geometry, loading and rigidity is addressed and numerical examples validate the effectiveness of the developed method. In Section 4, IGA is integrated with a developed semi-analytical sensitivity analysis technique for optimization and the validity of the optimization model is investigated using three examples. The pre-bending problem of wind turbine blades is addressed in this section as the third example. Finally, section 5 concludes the findings of the study.

2. Basic Definitions

B-spline curve algorithms which are required for implementing isogeometric analysis are briefly introduced in this section. The B-spline representations of geometry, load and rigidity which will be used throughout this paper are obtained through curve interpolation/approximation to be applicable in the real problem of pre-bending of wind turbine blade. Although NURBS are more general and more flexible than B-splines, there are further considerations and limitations in using NURBs in interpolation and approximation techniques [34-35], Therefore it was decided to choose B-splines in this paper.

2.1. B-spline curves and interpolation procedure

A clamped B-spline curve is a piecewise polynomial which is expressed by:

$$C(\xi) = \sum_{i=0}^{n} N_{i,p}(\xi) P_i \qquad (1)$$

where p is the degree and $P_i, i = 0, .., n$ is the control polygon defined by $P_i = (x_i, y_i, z_i)$. The term $N_{i,p}(\xi), i = 0, \dots, n$ represents B-spline basis functions that are defined on the knot vector, U given by:

$$U = \{\underbrace{0, \dots, 0}_{p+1}, u_{p+1}, \dots, u_{m-p-1}, \underbrace{1, \dots, 1}_{p+1}\} \qquad (2)$$

Outstanding properties and programming capabilities have made the B-spline curves popular for CAD/CAM/IGA applications. Three main steps employed in the current work for curve interpolation are as follows [31]:

a) Chord length parameterization

b) Knot vector generation using De-Boor algorithm

c) Calculating control points as the output of the problem

Parameters are in fact the reflection of distribution of data points. From Various parameterization techniques, Chord length parameterization which leads to linear parameterization [23, 36, 37, 38] is used. It should be noted that other parameterization techniques such as the equally spaced parameterization won't lead to linear or pseudo arc length parameterization. In this case, mesh distortion may occur and higher number of elements is needed to reach the desired convergence of the solution parameter.

If the input data points and their corresponding parameters are denoted by $Q_i, i = 0, \dots, k$, and $\xi_i, i = 0, \dots, k$, data point parameters are calculated by the chord length parameterization as:

$$\begin{cases} \xi_0 = 0 \\ \xi_i = \xi_{i-1} + \dfrac{|Q_i - Q_{i-1}|}{L} \\ \xi_k = 1 \end{cases} \qquad (3)$$

where

$$L = \sum_{i=1}^{k} |Q_i - Q_{i-1}|$$

Several methods are suggested for knot vector selection, amongst them the De-boor algorithm is preferred and implemented [31]:

$$\begin{gathered} d = \frac{k+1}{n-p+1} \\ i = int(jd) \quad , \quad \alpha = jd - i \\ u_{p+j} = (1-\alpha)\bar{u}_{i-1} + \alpha \bar{u}_i \quad , \quad j = 1, \dots, n-p \end{gathered} \qquad (4)$$

where *k* is the number of data points, *n* is the number of control points and *p* is the degree of B-spline. The "int" command gives the largest integer that is smaller than its input real number. The above algorithm will ensure that there is almost an equal number of parameters between the two consecutive knots which plays an important role in the stability of solutions and escaping the ill-conditioning issues of the stiffness matrices [39].

3. Isogeometric analysis of plane free-form beams

3.1. Stiffness Matrix and force vector

It is advantageous to use curvilinear coordinates and local bases for the description of free form curves as depicted in Fig. (2).

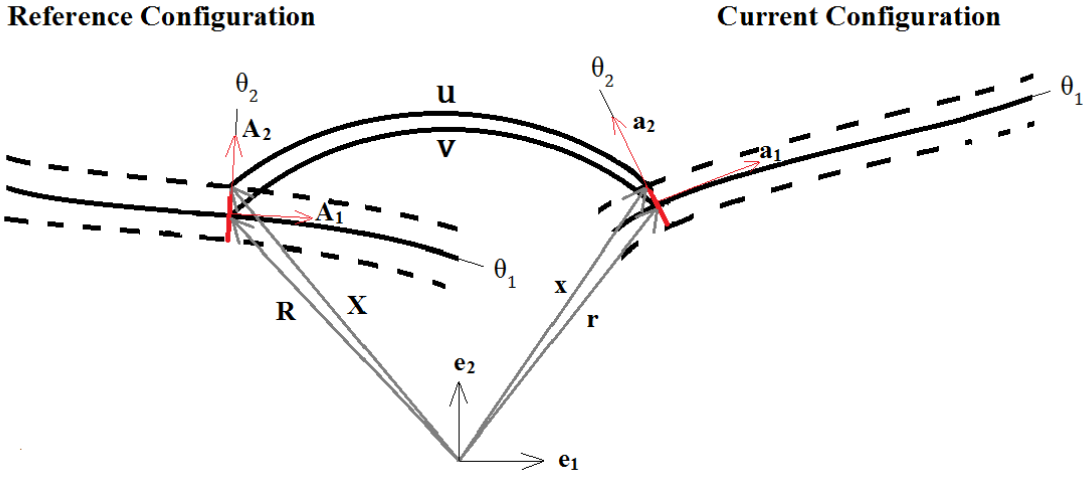

Figure 2 - Curved beam configurations in reference and deformed (current) states

In this Figure, $\boldsymbol{A}$ and $\boldsymbol{a}$ are the base vectors in reference and current configurations respectively. The deformation of a thin, elastic and uniform Euler-Bernoulli beam is comprised of membrane and flexural components. The plane position of each point on the deformed beam configuration (Fig. (3)) can be obtained using the following relation:

$$\boldsymbol{x}(\theta^1,\theta^2) = \boldsymbol{r}(\theta^1) + \theta^2 \boldsymbol{a_2}(\theta^1) \qquad (5)$$

where θ^1 and θ^2 are curvilinear coordinates and $\boldsymbol{r}$ is the position vector of the corresponding midline point.

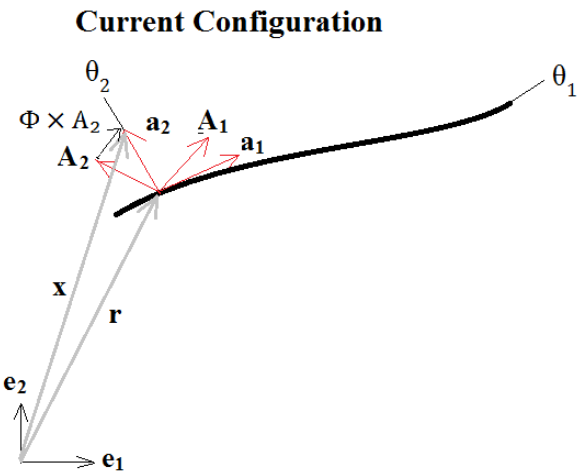

Figure 3 - A curvilinear configuration

The direction vector $\boldsymbol{a_2}$ can be written as:

$$\boldsymbol{a_2} = \boldsymbol{A_2} + \boldsymbol{\Phi} \times \boldsymbol{A_2} \tag{6}$$

where $\boldsymbol{\Phi}$ is the rotation vector. The rotation vector can be written as a function of rotation angle as:

$$\boldsymbol{\Phi} = \varphi_1 \boldsymbol{A_3} \tag{7}$$

where φ_1 is the rotation angle and can be calculated using the following equation:

$$\varphi_1 = \boldsymbol{\nu}_{,1}.\boldsymbol{A_2} \tag{8}$$

where $\boldsymbol{\nu_{,1}}$ is the partial derivative of midline displacement field, $\boldsymbol{\nu}$, with respect to the coordinate θ^1.

The difference between position vectors $\boldsymbol{x}$ and $\boldsymbol{X}$ will lead to a displacement field "$\boldsymbol{u}$" as:

$$\boldsymbol{u} = \boldsymbol{x} - \boldsymbol{X} \tag{9}$$

In derivation of the Green-Lagrange strain tensor coefficients, ε_{ij}, it is necessary to compute partial derivatives of the displacement field, $\boldsymbol{u}$, with respect to the coordinate θ^1:

$$\boldsymbol{u}_{,1} = \boldsymbol{\nu}_{,1} + \theta^2\left(\boldsymbol{\Phi}_{,1} \times \boldsymbol{A_2} + \boldsymbol{\Phi} \times \boldsymbol{A_{2,1}}\right) \tag{10}$$

The individual strain can be obtained using Green-Lagrange formula as:

$$\varepsilon_{11} = \boldsymbol{\nu}_{,1}\boldsymbol{A_1} + \theta^2\left(\boldsymbol{\nu}_{,1}\boldsymbol{A_{2,1}} + \boldsymbol{\Phi}_{,1} \times \boldsymbol{A_2}.\boldsymbol{A_1}\right) \tag{11}$$

The total potential energy, π, is the sum of the elastic strain energy, U, and the potential energy due to external forces, V. Considering energy minimization, the relation between external and internal virtual works is:

$$\delta\pi = \delta(U+V) = \int_{\Omega} \delta(\varepsilon)^T C\varepsilon d\Omega - \int_{S} \delta \boldsymbol{u}^T \boldsymbol{w} dS - \int_{\Omega} \delta \boldsymbol{u}^T \boldsymbol{f} dS = 0 \tag{12}$$

where **w** is the vector of distributed line loads, **f** is the vector of body forces and *C* is the material property coefficient.

In IGA, discretization is performed using B-spline basis functions. According to the isoparametric concept, the discrete displacement field of the midline, $\boldsymbol{v}$, is determined from basis functions defining the geometry and associated control points of the displacement field:

$$\boldsymbol{v}(\xi) = \sum_{i=1}^{n_{cp}} N_i^p(\xi)\ \boldsymbol{v}^i \tag{13}$$

where n_{cp} is the number of control points, ξ is the parameter, p is the B-spline degree, N_i^p are the basis functions, and $\boldsymbol{v}^i$ are control point values. $\boldsymbol{v}^i$ are the problem unknowns.

Since the vector $\boldsymbol{A_1}$ is always tangent to the curve, it can be written as:

$$\boldsymbol{A_1}(\xi) = \sum_{i=1}^{n_{cp}} N_i^P(\xi)_{,\xi}\, \boldsymbol{P}^i \tag{14}$$

where $\boldsymbol{P}^i$ are the control points of the input geometry. The stiffness matrix and force vector are computed by discretization of equation (12) using equations (10), (11), (13), and (14).

3.2. Analysis aware modeling in parameterizations of geometry, loading and rigidities

In a unified approach, the distributions of line loads and body forces have to be in the form of B-spline functions. The interpolation method which had been previously applied to geometry is similarly implemented for distributed loads/rigidities. It should be noted that the parameterization of the B-spline curve representing the distributed loading must be the same as that of geometry. In other words, the chord length parameterization of geometry introduced in Section 2, is directly assigned to load and rigidity. The one-to-one correspondence between parameters of loading and geometry is of extreme importance. Although the parameterization of geometry should be chord length (or linear), it is not the case for the parameterization of loading.

Independent parameterization for loading and geometry may change the definition of problem. To clarify this important issue, an illustrative example is provided in Fig. (4). Table (1) reports the values of B-spline parameters of geometry and load for independent and dependent cases. It should be mentioned that in the independent case, the parameterization of load (ξ_L) is obtained using equation (3). It can be seen that in the independent case, the values of ξ and ξ_L are not equal at a specified position, therefore, a unified parameter (ξ) will shift the load positions on the top of the beam. In this situation, the problem will be wrongly regarded as another problem with a different loading.

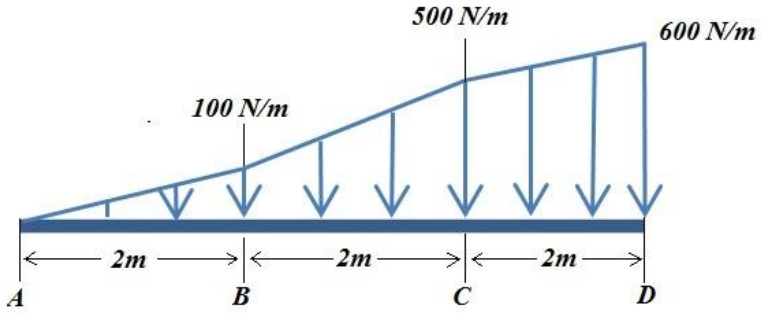

Figure 4 - A beam with 3-stage ramp loading

Table 1 - Values of B-spline parameters of geometry and load for the independent and dependent cases

Independent parameterization					Dependent parameterization				
Position	A	B	C	D	Position	A	B	C	D
Parameterization of geometry (ξ)	0	1/3	2/3	1	Parameterization of geometry (ξ)	0	1/3	2/3	1
Parameterization of load (ξ_L)	0	1/6	5/6	1	Parameterization of load (ξ_L)	0	1/3	2/3	1

The flexural rigidity of a curved-beam can vary along the length of the beam. The variation may be due to cross section changes (such as tapered beams), Young's modulus variations (composite materials) or both. A B-spline curve is capable of representing the flexural rigidity variations and can be directly implemented into IGA. The one-to-one correspondence between parameters of B-splines representing rigidity and geometry is again crucial here. Therefore, the B-spline representative of flexural rigidity variation is:

$$EI(\xi) = \sum_{i=1}^{n} N_i^p(\xi)\overline{EI}^i(\xi) \tag{15}$$

where $\overline{EI}^i$ are the interpolated control points. A similar procedure can be taken for the axial rigidity variation as:

$$EA(\xi) = \sum_{i=1}^{n} N_i^p(\xi)\overline{EA}^i(\xi) \tag{16}$$

3.3. Validation of Numerical Tests

Validation tests were conducted to ensure the effectiveness of the developed IGA formulation for free-form curves with arbitrarily load variations. The essential chord length parameterization method is used to assure the linearity of parameterization. In additions, the importance of one-to-one correspondence between parameterizations of load and geometry is discussed in details. It should be noted that in the following examples, the flexural/axial rigidities are assigned as constants.

Figs. (5) to (7) illustrate three examples along with the results obtained with IGA and FEM. In all cases, the cross section is circular with the diameter of 0.2 m. The modulus of elasticity is set equal to 200 GPa. The number of IGA and FE elements as well as the degree of shape/basis functions for a convergence up to 2 decimal points is reported in Table (2) for all examples. It should be noted that our objective is not to only compare IGA and FEM results, but is to ensure the validity of IGA formulations to be used in optimization problems where there are lots of deficiencies in implementing FE models [40].

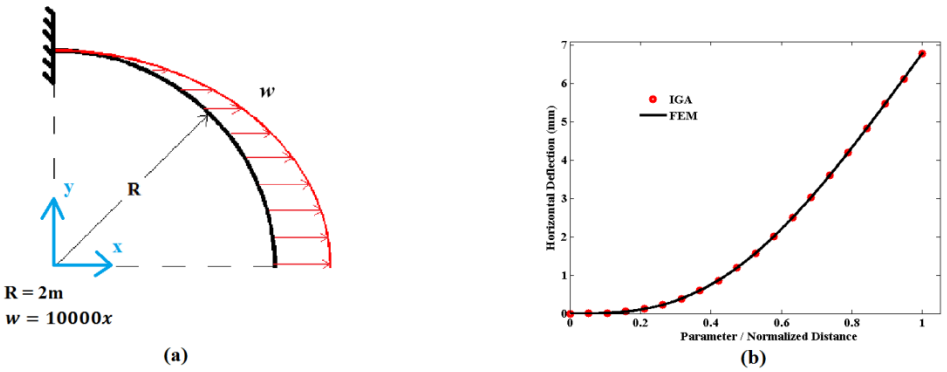

Figure 5 - (a) quadrant beam with variable horizontal loading (b) Comparing IGA and FEM results

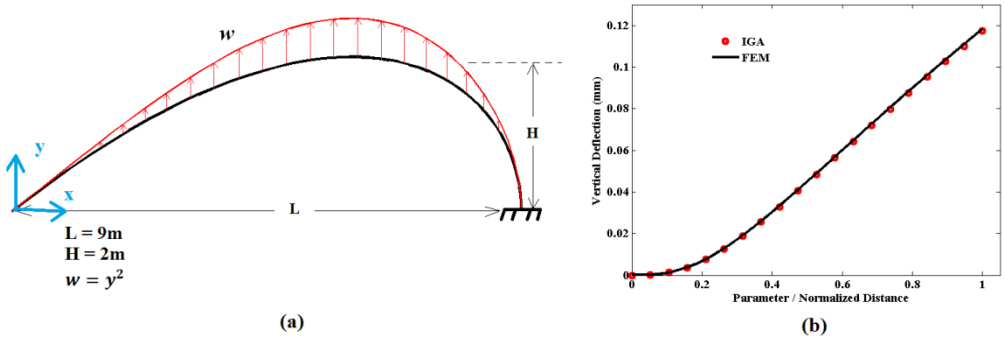

Figure 6 - (a) Tschirnhausen beam with variable vertical loading (b) Comparing IGA and FEM results

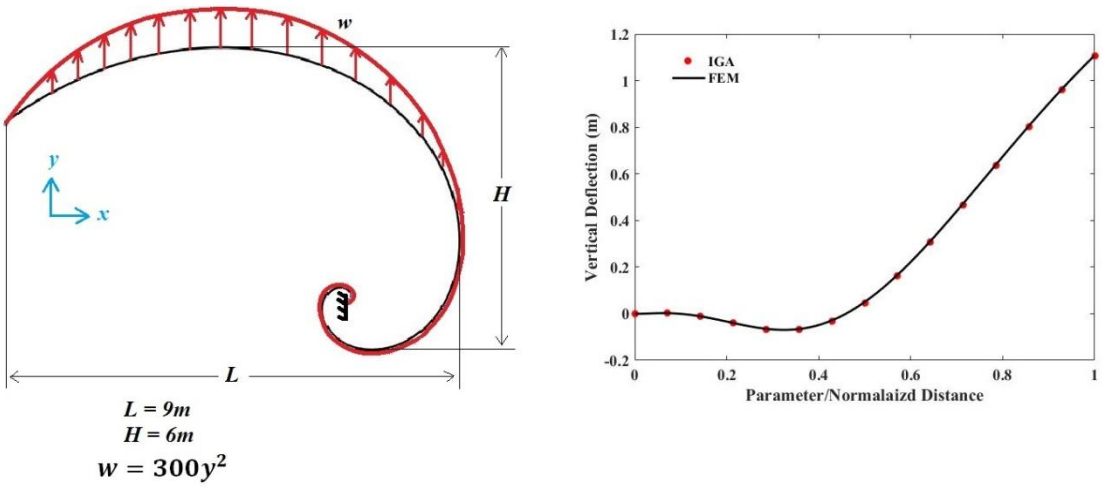

Figure 7 - (a) Spiral beam with variable vertical loading; (b) Comparing IGA and FEM results

Table 2 - The number of IGA and FE elements/degrees for a convergence up to 2 decimal points

Example	FEM		IGA	
	# of elements	Degree	# of elements	Degree
1 (Fig (5))	24	2	6	3
2 (Fig (6))	36	2	11	3
3 (Fig (7))	67	2	21	3

Comparing IGA and FEM results shows the validity of the IGA formulated method.

It is worth reminding here the relationship between parameterizations of the geometry and loading by a descriptive example. Based on the example depicted in Fig. (6), the variations of Jacobian versus B-spline parameter for the geometry and loading are taken into consideration and presented in Fig. (8).

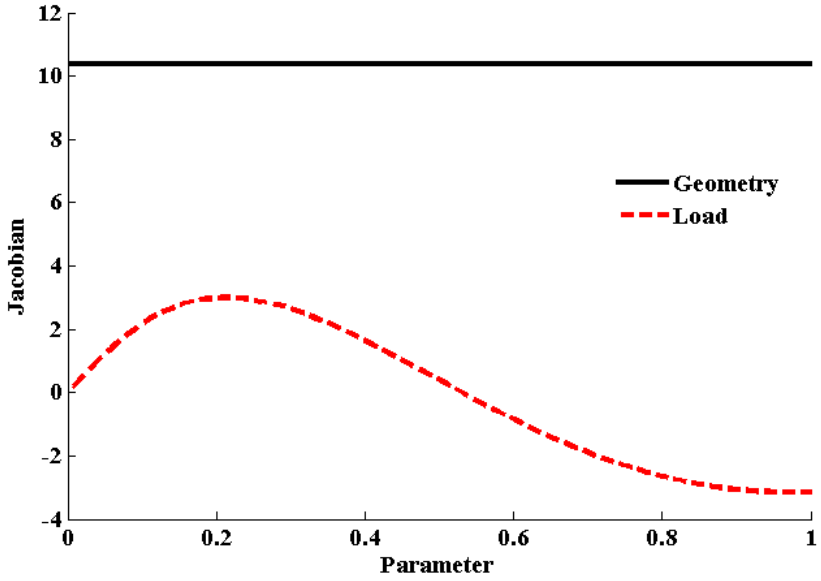

Figure 8 - The variation of Jacobian with respect to B-spline parameter for geometry and load of Fig. (6-a)

This figure illustrates that the parameterization of geometry is linear (constant Jacobian), while the parameterization of load, which is correctly adopted from the geometry, is not linear. Therefore, employing an independent linear parameterization for loading in this example seriously affects the accuracy of results.

4. Formulation of the Shape/Flexural Rigidity Optimization

4.1. Optimization procedure

For a linear elastic body, the aim of shape optimization is to find the shape of a domain which minimizes an objective function. The optimization problem may be expressed as:

$$\min_{\Omega \subseteq D} F(x)$$

subject to:

$$h_j(x) = 0, \quad j = 1, 2 \dots n_h$$

$$q_k(x) \leq 0, \quad k = 1,2 \dots n_k$$

where$D \subseteq R^2$ denotes the set of admissible shapes defined through the local geometric constraints. Design variables defining the shape are denoted by x_i $(i = 1, \dots, n)$ while h_j and q_k are the equality and inequality constraints respectively. The objective function, F(x), can be volume, weight, strain energy, or stress.

Among various optimization strategies developed for shape optimization problems, the superiority of gradient-based optimization methods have been underscored by many researchers [41, 42]. Gradient-based algorithms seek to iteratively update the design variables based on the results of sensitivity analyses. The sensitivity analysis addresses how much the variation of a design variable will affect the objective function and what is the update direction for function minimization.

In this paper, Sequential Quadratic Programming (SQP) is used as the optimization tool in sensitivity analysis. In SQP optimization with only inequality constraints, all information related to the problem are incorporated into the Lagrangian functional as:

$$L = f(x) + \lambda^T q(x) \tag{17}$$

where λ are Lagrangian multipliers.

The Karush-Kuhn-Tucker condition is obtained by imposing the well-known Newtons method on the Lagrangian function which takes the following matrix form:

$$\begin{bmatrix} H & G^T \\ G & 0 \end{bmatrix} \begin{bmatrix} -\bar{\mathbf{P}} \\ \boldsymbol{\lambda}^{k+1} \end{bmatrix} = \begin{bmatrix} \mathbf{g} \\ \mathbf{q} \end{bmatrix} \tag{18}$$

where $\bar{\mathbf{P}} = \frac{\mathbf{x}^{k+1} - \mathbf{x}^{k}}{\alpha}$, $G = \boldsymbol{\nabla}_x \mathbf{q}$, $g = \boldsymbol{\nabla}_x F$, $H = \boldsymbol{\nabla}_{xx}^2 F$, α is the step length and λ^{k+1} are the updated Lagrangian multipliers. The analytical calculation of the Hessian matrix (H) is not possible in the present work. Therefore, the Hessian matrix is approximated using the Symmetric Rank-one (SRI) quasi Newton iteration method as:

$$H^{k+1} = H^{k} + \frac{(\boldsymbol{\nabla}\mathbf{g} - H^{k}\boldsymbol{\nabla}\mathbf{x})(\boldsymbol{\nabla}\mathbf{g} - H^{k}\boldsymbol{\nabla}\mathbf{x})^{T}}{(\boldsymbol{\nabla}\mathbf{g} - H^{k}\boldsymbol{\nabla}\mathbf{x})^{T}\boldsymbol{\nabla}\mathbf{x}} \tag{19}$$

The values of x^{k+1} are updated iteratively by solving equation (18). It should be mentioned that the value of α is chosen based on the feasibility conditions of the updated design variables. The simplest method of calculating the gradient of objective function with respect to each design variable is the global finite difference method:

$$\boldsymbol{\nabla} f(x_i) = \frac{f(x_1, x_2, \dots, x_i + \varepsilon, \dots, x_n) - f(x_1, x_2, \dots, x_i, \dots, x_n)}{\varepsilon} \tag{20}$$

where ε is a disturbance parameter. The convergence of global finite difference method is highly dependent on the disturbance parameter and it is an inefficient method in many applications [43]. One reliable alternative is the semi-analytical sensitivity analysis method which is based on the direct manipulation of the derivatives. The objective function of a shape optimization problem aiming at pre-bent shape design is:

$$OF = \left[\mathbf{CP}_{\mathbf{pre-bent}} + \mathbf{CP}_{\mathbf{disp}} - \mathbf{CP}_{\mathbf{prescribed}}\right]^{T}\left[\mathbf{CP}_{\mathbf{pre-bent}} + \mathbf{CP}_{\mathbf{disp}} - \mathbf{CP}_{\mathbf{prescribed}}\right] \tag{21}$$

where $\mathbf{CP}_{\mathbf{pre-bent}}$ are control point positions of the design variables at each iteration step, $\mathbf{CP}_{\mathbf{disp}}$ are control points of the displacement field (v^i in equation (13)), and $\mathbf{CP}_{\mathbf{prescribed}}$ are the required deflected positions of control points after loading (constant input values).

The derivative of objective function with respect to the design variable, x_i, can be formulated as:

$$\frac{\partial OF}{\partial x_i} = 2 * \left[\mathbf{CP}_{\mathbf{pre-bent}} + \mathbf{CP}_{\mathbf{disp}} - \mathbf{CP}_{\mathbf{prescribed}}\right]^{T}\left(\boldsymbol{\delta} + \frac{\partial \mathbf{CP}_{\mathbf{disp}}}{\partial x_i}\right) \tag{22}$$

where δ is a vertical vector which all of its members are zero except for the i^{th} member which equals 1.

The derivative of displacement control points with respect to the design variable, x_i, is obtained by deriving the equilibrium equation:

$$\frac{d}{dx_i}\left\{[K]\{\mathbf{CP}_{\mathbf{disp}}\}\right\} = \frac{d}{dx_i}\{\mathbf{f}\} \tag{23}$$

Therefore

$$\frac{d\,\mathbf{CP}_{\mathbf{disp}}}{dx_i} = [K]^{-1}\left(\left\{\frac{\partial \mathbf{f}}{\partial x_i}\right\} - \left[\frac{\partial K}{\partial x_i}\right]\{\mathbf{CP}_{\mathbf{disp}}\}\right) = [K]^{-1}\{\mathbf{f}^{*}\} \tag{24}$$

$\mathbf{f}^{*}$ is called the Pseudo load vector and is defined as:

$$\{\mathbf{f}^{*}\} = \left\{\frac{\partial \mathbf{f}}{\partial x_i}\right\} - \left[\frac{\partial K}{\partial x_i}\right]\{\mathbf{CP}_{\mathbf{disp}}\} \tag{25}$$

The derivative $\frac{\partial \mathbf{f}}{\partial x_i}$ is usually zero since the applied force is almost independent of design variables whereas the derivative of stiffness matrix with respect to the design variables ($\frac{\partial K}{\partial x_i}$) is frequently approximated by the global finite difference method. Semi-analytically computation of the Pseudo load vector requires only computing the stiffness matrix of the perturbed system, meaning that no mapping from the analytical model to the design model is required [41].

In shape optimization of curved beams, the control points defining the beam's shape are taken as design variables. Although global optimization methods such as PSO are very suitable for the selection of the initial design, especially when the derivatives of the objective function are unknown [44], in the pre-bending shape design problems, it is advantageous to use the deflected values ($\mathbf{CP_{prescribed}}$) as the initial guess. This is because the deflected configuration is somehow similar to the pre-bent configuration in curvature variations and visual appearance, therefore, the values of $\mathbf{CP_{prescribed}}$ are selected as the initial guess for all subsequent optimization examples. In the present work, inequality constraints are emerged as limit bounds as will be shown in the following examples.

4.2. Optimization Examples

The following examples are used to ensure the validity of semi-analytical optimization method developed in the current research.

4.2.1. Pre-bent shape design of cantilever Tschirnhausen beam

In order to solve the pre-bent design of a curved beam using the optimization algorithm, the control points of the geometry (Fig. (9)) are allowed to move in horizontal and vertical directions throughout the design space.

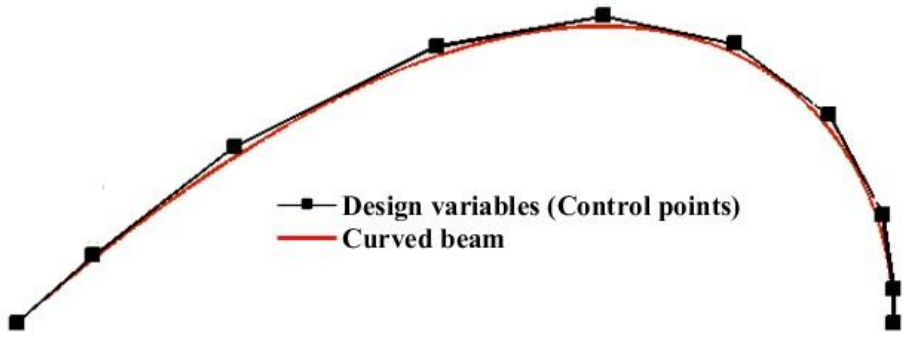

Figure 9 - Control points of the Tschirnhausen curve as optimization design variables

The geometry and configuration of loading are as previously shown in Fig. (6.a), but the magnitude of distributed load is $w = 5000y^2$ in the current example. The Semi-analytical technique is performed to

find out the control points of the pre-bent configuration. The optimization input parameters of this example are listed in Table (3).

Table 3 - Optimization parameters of the pre-bending of Tschirnhausen's example

Initial step length $[\alpha]$	Initial Hessian $[H]$	Disturbance parameter of finite difference method (ε)	Optimization formulation	Selection of initial design	Design space
1	Identity matrix	0.001	Acc. to section 4	Equals to $\boldsymbol{CP}_{\boldsymbol{prescribed}}$	Bounded $x \in [-10,10]$ $y \in [-10,10]$

The convergence histories of the semi-analytical technique using IGA and FEM as structural analysis tools are demonstrated in Fig. (10). High convergence rate (only 9 iterations to reach an objective function value of lower than 10^{-4}) can be seen in the IGA case. The superiority of IGA with respect to FEM is clearly observed. It is worth noting that the time required for each iteration with FEM is 4 times greater than that of IGA, a fact which comes from lower number of design variables for accuracy requirements in IGA compared to FEM (see Table (2)).

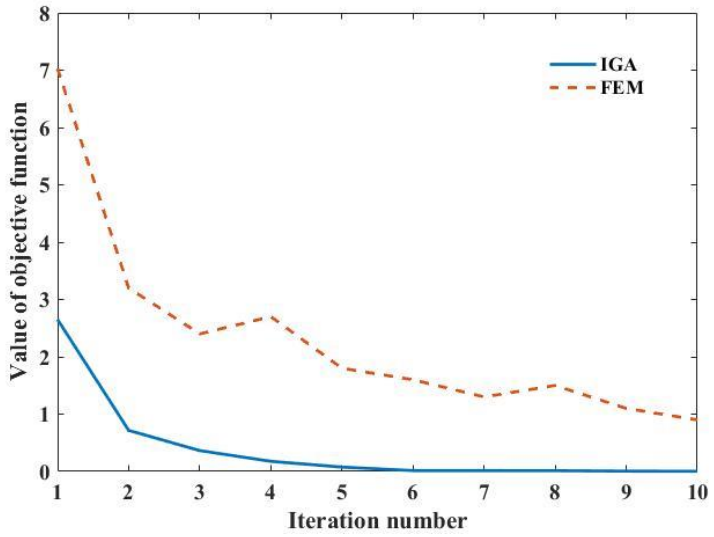

Figure 10 – iterative history of example 1

The pre-bending results are shown in Fig. (11). The deflected curve is closely lying on the required deformed geometry. Therefore, the proposed technique can predict the pre-bent shape of free-form curves under arbitrary distributed loading accurately.

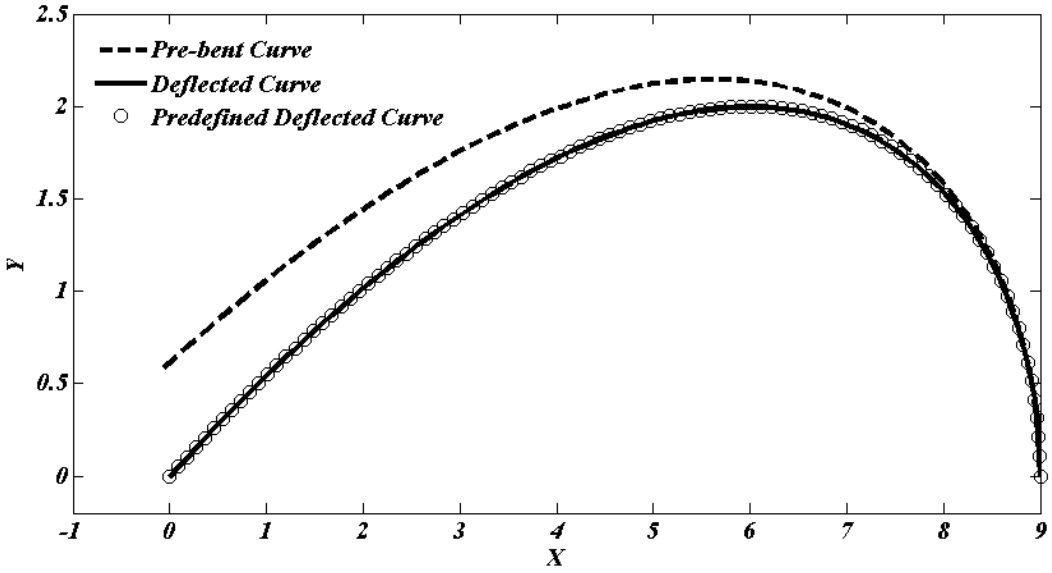

Figure 11 –Pre-bent shape design of the Tschirnhausen curved beam

4.2.2. Pre-bent shape design of cantilever spiral beam

Spiral shapes are of important and complicated planar curved beams that are widely used in engineering applications. In this section, the pre-bent shape design of a spiral beam is considered. The geometry and control polygon of the problem is shown in Fig. (12). All control points are allowed to move freely in both x and y directions inside the design space. The geometry and loading are the same as Fig. (7.a), but the direction of the distributed load is reversed. All necessary information related to the optimization problem of this example is listed in Table (4).

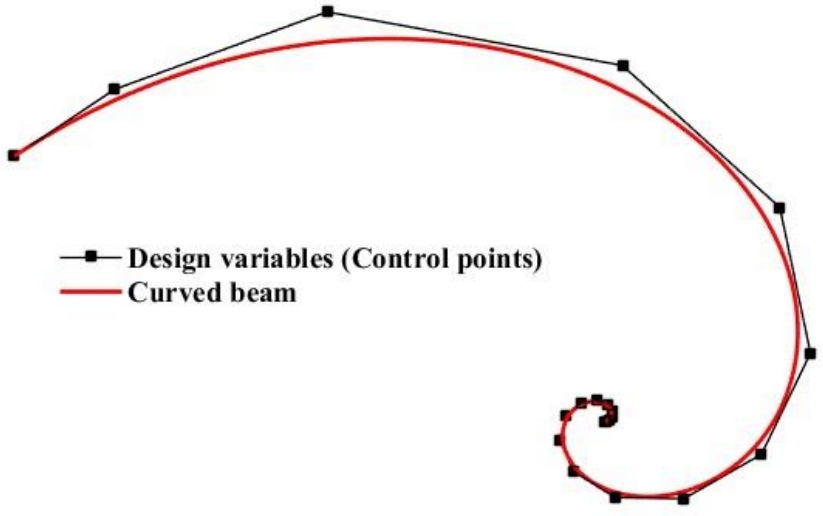

Figure 12 - Control points of the Spiral curve as optimization design variables

Table 4 - Optimization parameters of the pre-bending of Spiral's example

Initial step length $[\alpha]$	Initial Hessian $[H]$	Disturbance parameter of finite difference method (ε)	Optimization formulation	Selection of initial design	Design space
1	Identity matrix	0.001	Acc. to section 4	Equals to $\boldsymbol{CP}_{\boldsymbol{prescribed}}$	Bounded $x \in [-10,10]$ $y \in [-10,10]$

Fig. (13) shows the convergence history of the objective function with respect to the iteration number. Good convergence is shown which is promising. The superiority of IGA with respect to FEM is again observed. In this example, the average time required for each iteration with IGA is 9 times faster than the average time required for each iteration step with FEM. The pre-bending results are shown in Fig. (14) for comparison purposes. The deflected and predefined configurations are matched well indicating that the predicted pre-bent curve is well-designed.

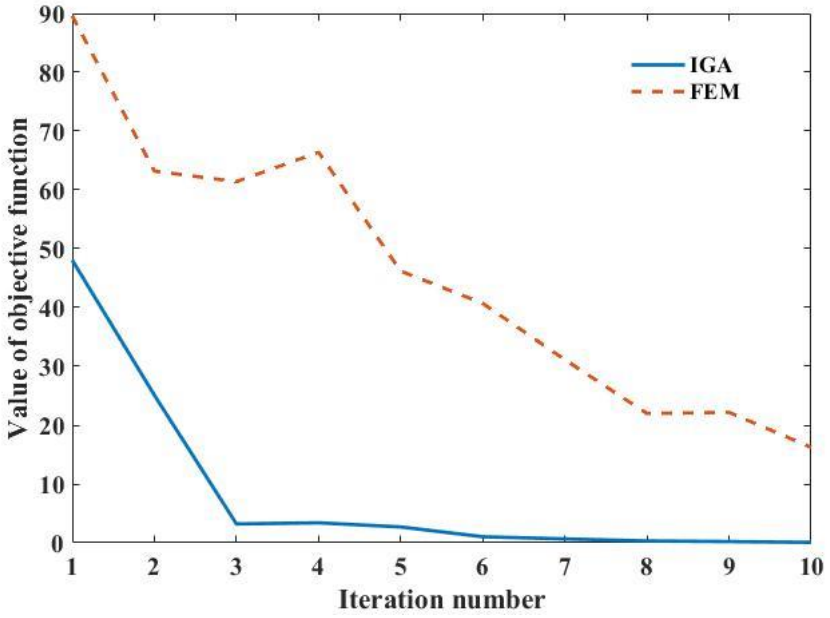

Figure 13 -The iteration history of example 2

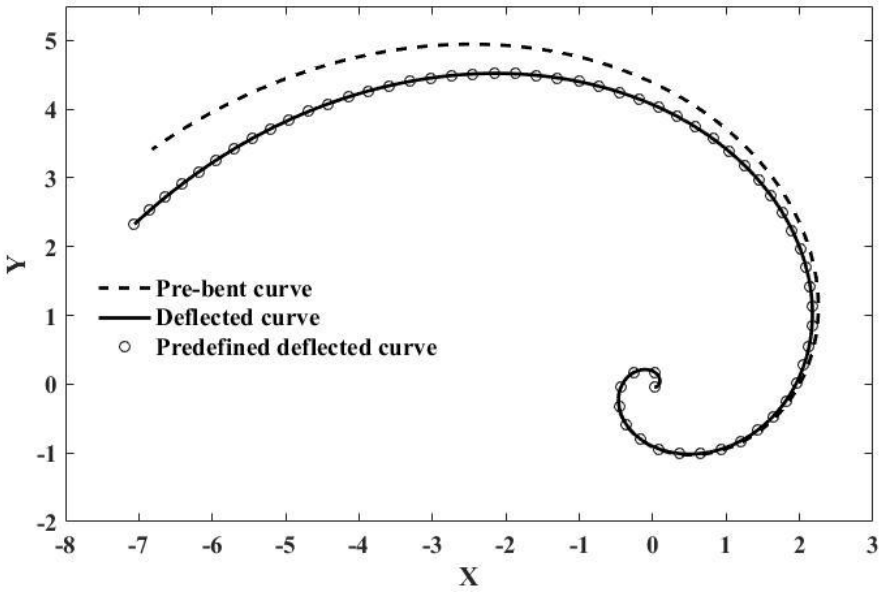

Figure 14 - Pre-bent shape design of the Spiral curved beam

4.2.3. Pre-bending of Wind Turbine Blades (a practical example)

The wind turbine blade design, in terms of functionality, can be divided into structural and aerodynamic areas [45, 46]. The main objective of aerodynamic design is to convert the kinetic energy of wind into differential lift and drag forces which eventually result in the main shaft torsional moment. On the other hand, the objective of structural analysis is to design the composite layup to sustain large amount of bending moments which are maximized on the blade root. Large deflection is the main concern and the critical issue in structural (Layup) design of composite wind turbine blades. Although composite materials have considerable amount of strength, their stiffness is not very high. Therefore, such composite structures may undergo large deflections during operational and extreme conditions. Large deflection of typical wind turbine blades is the source of many design problems. The blades have to be stiff enough so that they don't hit the tower under extreme wind conditions. There are some practices to raise the clearance safety factor without sacrificing the material and cost such as defining a cone angle, a tilt angle, and pre-bending. These are shown schematically in Fig. (15).

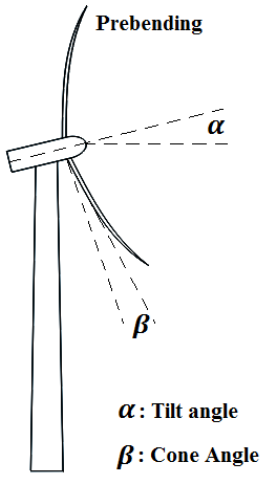

Figure 15- Practical methods of increasing the tower clearance

A Cone angle of 3^{o}, Tilt angle of 5^{o} and 1.5 m pre-bending for a 50 meters wind turbine blade are common figures [47]. It is obvious that allocating cone and tilt angles needs some adjustment in the design of nacelle, but pre-bending is implemented in the mold design of the blade itself. The pre-bent blades are bent toward the wind. When the blades are exposed to the wind loads, they become straight which is their best configuration based on aerodynamic considerations. Hence, pre-bending allows the blades to be longer and lighter with larger swept area [48]. The required pre-bent configuration can be obtained using the optimization method introduced in this paper.

In this section, the introduced IGA-SQP semi-analytical optimization procedure was performed on a 13m wind turbine blade. The flapwise aerodynamic load on the beam representing the blade is computed using FAST [49]. The blade's structure consists of glass-epoxy composites in its shell and spar. The variation of flexural and axial rigidities along the blade is obtained using Precomp [50]. In the next step, the blade's initial geometry, loading, and rigidities are interpolated using the method described in Section 2. The results for an example of 10 control points and degree 3 are shown in Fig. (16). The optimization input parameters of this example are listed in Table (5).

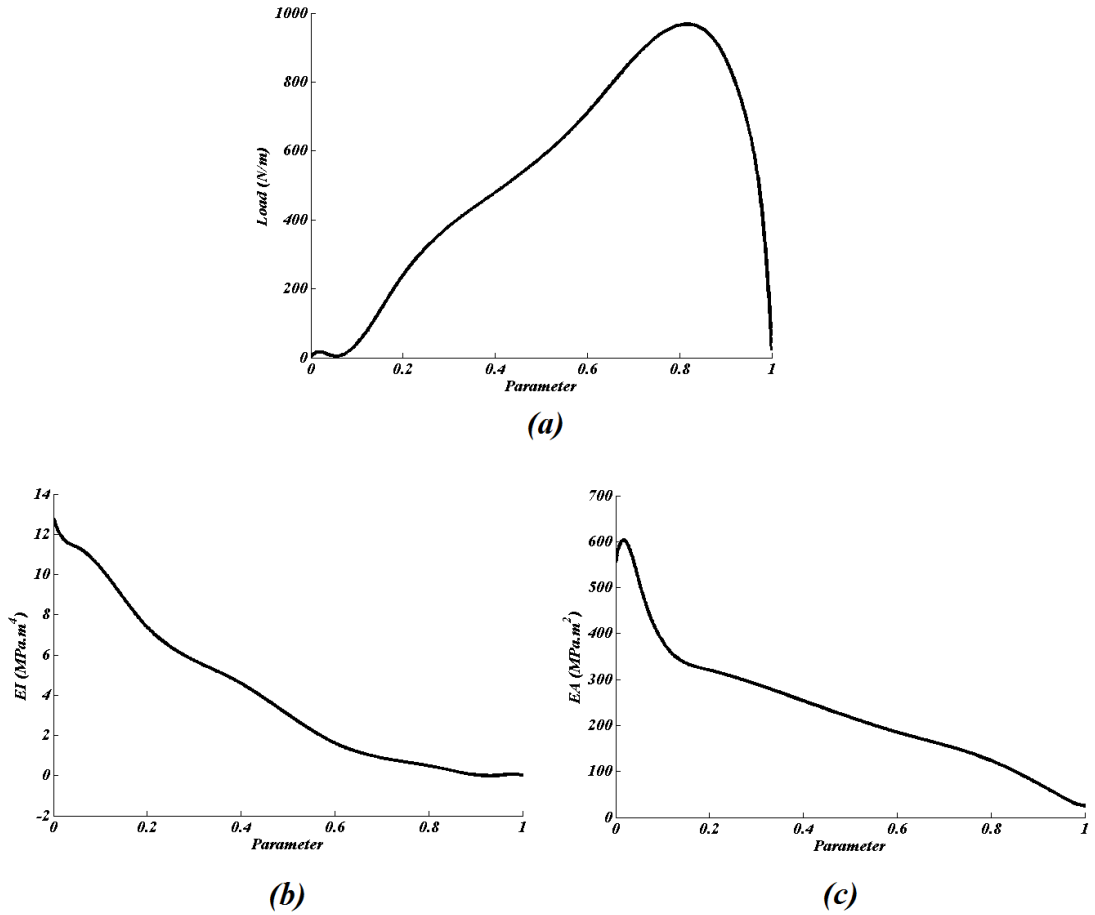

Figure 16 - The variation of (a) load, (b) flexural rigidity and (c) axial rigidity with respect to the B-spline parameter

Table 5 - Optimization parameters of the pre-bending of wind turbine blade example

Initial step length [α]	Initial Hessian [H]	Disturbance parameter of finite difference method (ε)	Optimization formulation	Selection of initial design	Design space
0.25	Identity matrix	0.0001	Acc. to section 4	Equals to $\boldsymbol{CP}_{\boldsymbol{prescribed}}$	Bounded $x \in [-15,15]$ $y \in [-15,15]$

The control points of geometry (except for the fixed end) are given freedom to move vertically and create different curved beams. The convergence study of the proposed semi-analytical procedure and the final pre-bent shape are shown in Figs. (17) and (18) respectively.

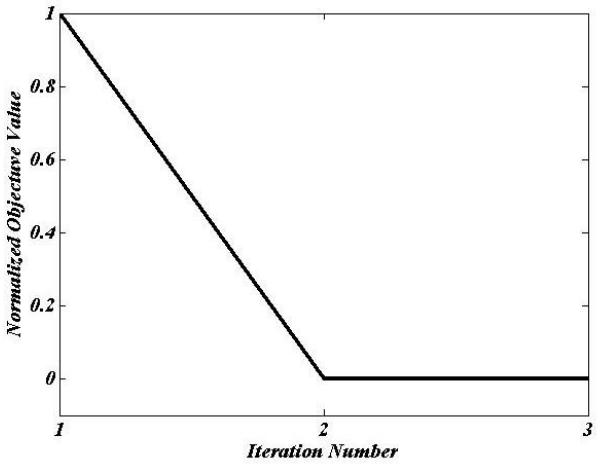

Figure 17 – Iterative history of wind turbine blade's pre-bending example

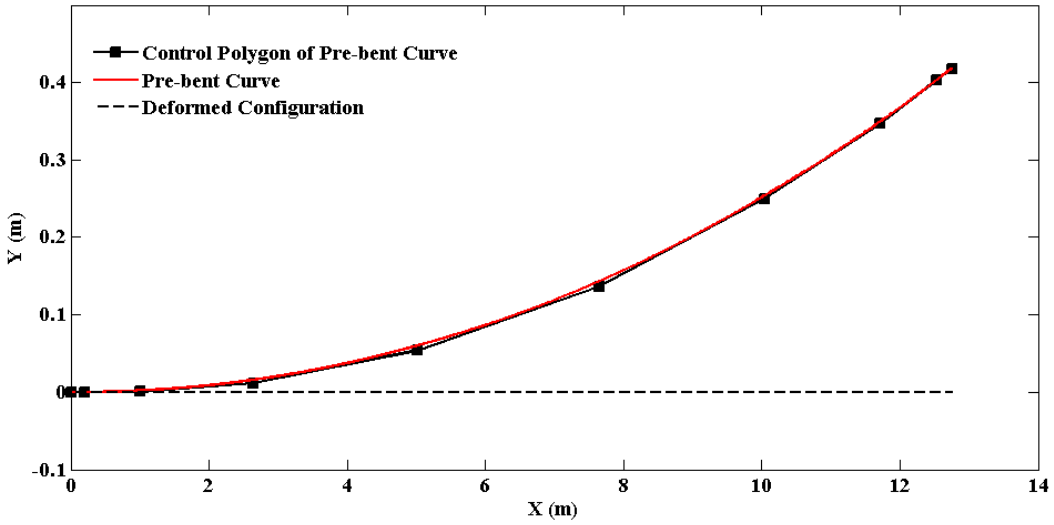

Figure 18 – The Pre-bent shape of a wind turbine blade using semi-analytical optimization

According to Fig. (17), the normalized objective function converged to a number below the required accuracy (10^{-5} in this article) in only 3 iterations. The straight deformed configuration in Fig. (18) confirms the validity of the pre-bent shape designed. Fig. (18) also illustrates that for the present example, a maximum tip pre-bending of approximately 0.4 m is sufficient.

Finally, a convergence study has been conducted to investigate the effect of number of design variables on the convergence of the objective function value which is shown in Fig. (19).

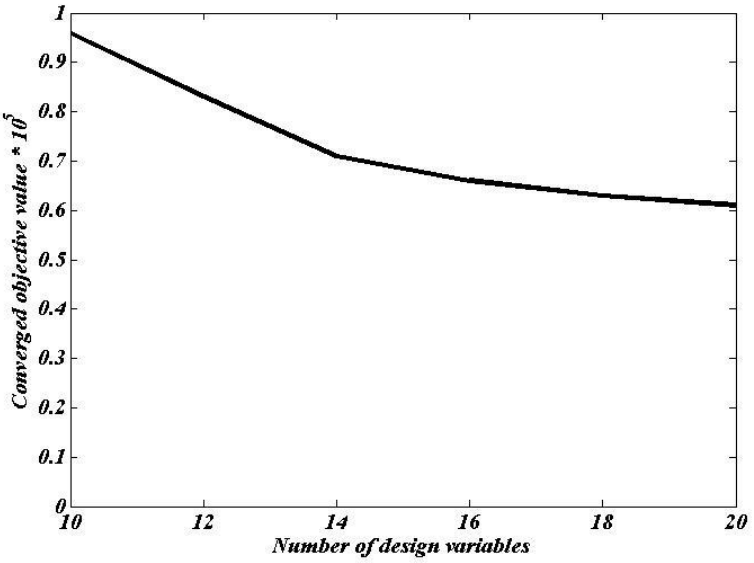

Figure 19 - The effect of number of design variables on the converged objective value of the wind turbine blade example

The figure suggests that slightly better results are obtained by increasing the number of control points from 10 to 20 using the knot insertion algorithm [31]. Nevertheless, 10 control points can be also sufficient for this example.

1. Conclusion

In this paper, the isogeometric analysis formulation of a curved beam with free-form geometry, arbitrary loading and variable flexural/axial rigidity is presented. It is shown that the parameterization of the loading/rigidity should be the same as the parameterization of the geometry. The tried and tested chord-length parameterization is used for parameterization of the curved beam geometry. The B-spline representations of geometry, loading and rigidity are constructed using the interpolation technique. The results obtained by IGA of curved beam models are verified by refined FEA solutions. Isogeometric analysis is then profitably integrated with the semi-analytical sensitivity analysis to solve pre-bent shape design problems. As an industrial example, the proposed optimization method is successfully employed in the pre-bent shape design of composite wind turbine blades under distributed aerodynamic loading. Finally, much remains to be done in order to extend the presented optimization methodology to bivariate problems like shells, which can be suggested as a future work.

References

1. Imam, M.H., Three-dimensional shape optimization. International Journal for Numerical Methods in Engineering, 1982. 18(5): p. 661-673.
2. Choi, J.-H., Shape design sensitivity analysis and optimization of general plane arch structures. Finite Elements in Analysis and Design, 2002. 39(2): p. 119-136.
3. Daxini, S.D. and J.M. Prajapati, Parametric shape optimization techniques based on Meshless methods: A review. Structural and Multidisciplinary Optimization, 2017. 56(5): p. 1197-1214.
4. Hughes, T.J.R., J.A. Cottrell, and Y. Bazilevs, Isogeometric analysis: CAD, finite elements, NURBS, exact geometry and mesh refinement. Computer Methods in Applied Mechanics and Engineering, 2005. 194(39–41): p. 4135-4195.
5. Hosseini, S.F., Hashemian, A., Moetakef-Imani, B., Hadidimoud, S., Isogeometric Analysis of Free-form Timoshenko Curved Beams Including the Nonlinear Effects of Large Deformations, Acta Mechanica Sinica, (in press).
6. Ghafari, E. and J. Rezaeepazhand, Isogeometric analysis of composite beams with arbitrary cross-section using dimensional reduction method. Computer Methods in Applied Mechanics and Engineering, 2017. 318: p. 594-618.
7. Cottrell, J.A., et al., Isogeometric analysis of structural vibrations. Computer Methods in Applied Mechanics and Engineering, 2006. 195(41–43): p. 5257-5296.
8. Bazilevs, Y. and T.J.R. Hughes, Weak imposition of Dirichlet boundary conditions in fluid mechanics. Computers & Fluids, 2007. 36(1): p. 12-26.
9. Ghaffari Motlagh, Y., et al., Simulation of laminar and turbulent concentric pipe flows with the isogeometric variational multiscale method. Computers & Fluids, 2013. 71: p. 146-155.
10. Yoon, M., S.-H. Ha, and S. Cho, Isogeometric shape design optimization of heat conduction problems. International Journal of Heat and Mass Transfer, 2013. 62: p. 272-285.
11. Wang, D., Q. Liang, and H. Zhang, A superconvergent isogeometric formulation for eigenvalue computation of three dimensional wave equation. Computational Mechanics, 2016: p. 1-24.
12. Hao, P., et al., Isogeometric buckling analysis of composite variable-stiffness panels. Composite Structures, 2017. 165(Supplement C): p. 192-208.
13. Cho, S. and S.-H. Ha, Isogeometric shape design optimization: exact geometry and enhanced sensitivity. Structural and Multidisciplinary Optimization, 2008. 38(1): p. 53.
14. Fußeder, D., B. Simeon, and A.V. Vuong, Fundamental aspects of shape optimization in the context of isogeometric analysis. Computer Methods in Applied Mechanics and Engineering, 2015. 286: p. 313-331.
15. Taheri, A.H. and B. Hassani, Simultaneous isogeometrical shape and material design of functionally graded structures for optimal eigenfrequencies. Computer Methods in Applied Mechanics and Engineering, 2014. 277: p. 46-80.
16. Qian, X., Topology optimization in B-spline space. Computer Methods in Applied Mechanics and Engineering, 2013. 265: p. 15-35.
17. Taheri, A.H., B. Hassani, and N.Z. Moghaddam, Thermo-elastic optimization of material distribution of functionally graded structures by an isogeometrical approach. International Journal of Solids and Structures, 2014. 51(2): p. 416-429.
18. Seo, Y.-D., H.-J. Kim, and S.-K. Youn, Isogeometric topology optimization using trimmed spline surfaces. Computer Methods in Applied Mechanics and Engineering, 2010. 199(49–52): p. 3270-3296.
19. Bauer, A.M., et al., Nonlinear isogeometric spatial Bernoulli beam. Computer Methods in Applied Mechanics and Engineering, 2016. 303: p. 101-127.

20. Bouclier, R., T. Elguedj, and A. Combescure, Locking free isogeometric formulations of curved thick beams. Computer Methods in Applied Mechanics and Engineering, 2012. 245–246: p. 144-162.
21. Cazzani, A. and M. Malagu, Isogeometric Analysis of Plane-Curved Beam. Mathematics and Mechanics of Solids, 2014. 1-16.
22. Wang, D., W. Liu, and H. Zhang, Superconvergent isogeometric free vibration analysis of Euler–Bernoulli beams and Kirchhoff plates with new higher order mass matrices. Computer Methods in Applied Mechanics and Engineering, 2015. 286: p. 230-267.
23. Kolman, R., et al., Isogeometric analysis of free vibration of simple shaped elastic samplesa). The Journal of the Acoustical Society of America, 2015. 137(4): p. 2089-2100.
24. Weeger, O., U. Wever, and B. Simeon, Isogeometric analysis of nonlinear Euler–Bernoulli beam vibrations. Nonlinear Dynamics, 2013. 72(4): p. 813-835.
25. Hongliang Liu, Xuefeng Zhu, and D. Yang, Isogeometric method based in-plane and out-of-plane free vibration analysis for Timoshenko curved beams. Structural Engineering and Mechanics, 2016. 59(3).
26. Luu, A.-T., N.-I. Kim, and J. Lee, Bending and buckling of general laminated curved beams using NURBS-based isogeometric analysis. European Journal of Mechanics - A/Solids, 2015. 54: p. 218-231.
27. Wang, X., X. Zhu, and P. Hu, Isogeometric finite element method for buckling analysis of generally laminated composite beams with different boundary conditions. International Journal of Mechanical Sciences, 2015. 104: p. 190-199.
28. Nagy, A.P., M.M. Abdalla, and Z. Gürdal, Isogeometric sizing and shape optimisation of beam structures. Computer Methods in Applied Mechanics and Engineering, 2010. 199(17–20): p. 1216-1230.
29. Nagy, A.P., M.M. Abdalla, and Z. Gürdal, Isogeometric design of elastic arches for maximum fundamental frequency. Structural and Multidisciplinary Optimization, 2010. 43(1): p. 135-149.
30. E. Cohen, T. Martin, R.M. Kirby, T. Lyche, R.F. Riesenfeld, Analysis-aware modeling: Understanding quality considerations in modeling for isogeometric analysis, Computer Methods in Applied Mechanics and Engineering, 199 (2010) 334-356.
31. Piegl, L. and W. Tiller, The NURBS book (2nd ed.). 1997: Springer-Verlag New York, Inc. 646.
32. A. Hashemian, B.M. Imani, A New Quality Appearance Evaluation Technique for Automotive Bodies Including Effect of Flexible Parts Tolerances, Mechanics Based Design of Structures and Machines, (2017) 1-11.
33. Choi, M.-J., M. Yoon, and S. Cho, Isogeometric configuration design sensitivity analysis of finite deformation curved beam structures using Jaumann strain formulation. Computer Methods in Applied Mechanics and Engineering, 2016. 309(Supplement C): p. 41-73.
34. Park, H., K. Kim, and S.C. Lee, A method for approximate NURBS curve compatibility based on multiple curve refitting. Computer-Aided Design, 2000. 32(4): p. 237-252.
35. B.M. Imani, S.A. Hashemian, NURBS-Based Profile Reconstruction using Constrained Fitting Techniques, Journal of Mechanics, 28 (2012) 407-412.
36. Kolman, R., J. Plešek, and M. Okrouhlík, Complex wavenumber Fourier analysis of the B-spline based finite element method. Wave Motion, 2014. 51(2): p. 348-359.
37. Hosseini, S.F., et al., The effect of parameterization on isogeometric analysis of free-form curved beams. Acta Mechanica, 2016: p. 1-16.
38. A. Hashemian, S.F. Hosseini, S.N. Nabavi, Kinematically Smoothing Trajectories by NURBS Reparameterization – An Innovative Approach, Advanced Robotics, 2017. 36.
39. Park, H. and K. Kim, Smooth surface approximation to serial cross-sections. Computer-Aided Design, 1996. 28(12): p. 995-1005.

40. Seo, Y.-D., H.-J. Kim, and S.-K. Youn, Shape optimization and its extension to topological design based on isogeometric analysis. International Journal of Solids and Structures, 2010. 47(11): p. 1618-1640.
41. Kiendl, J., et al., Isogeometric shape optimization of shells using semi-analytical sensitivity analysis and sensitivity weighting. Computer Methods in Applied Mechanics and Engineering, 2014. 274: p. 148-167.
42. Qian, X., Full analytical sensitivities in NURBS based isogeometric shape optimization. Computer Methods in Applied Mechanics and Engineering, 2010. 199(29): p. 2059-2071.
43. Laporte, E. and P.L. Tallec, Numerical Methods in Sensitivity Analysis and Shape Optimization. 2013: Birkh.
44. Campana, E.F., et al., Initial Particles Position for PSO, in Bound Constrained Optimization, in Advances in Swarm Intelligence: 4th International Conference, ICSI 2013, Harbin, China, June 12-15, 2013, Proceedings, Part I, Y. Tan, Y. Shi, and H. Mo, Editors. 2013, Springer Berlin Heidelberg: Berlin, Heidelberg. p. 112-119.
45. Hosseini, S.F. and B. Moetakef-Imani, Improved B-Spline Skinning Approach for Design of Hawt Blade Mold Surfaces. Journal of Mechanics, 2016. 33(4): p. 427-433.
46. Hosseini, S.F. and B. Moetakef-Imani, Innovative approach to computer-aided design of horizontal axis wind turbine blades. Journal of Computational Design and Engineering, 2017. 4(2): p. 98-105.
47. Burton, T., et al., Wind Energy Handbook. 2011, John Wiley & Sons, Ltd.
48. Bazilevs, Y., et al., A computational procedure for prebending of wind turbine blades. International Journal for Numerical Methods in Engineering, 2012. 89(3): p. 323-336.
49. Jonkman, J.M. and M.L. Buhl, FAST User's Guide. 2005, National Renewable Energy Laboratory: Golden, Colorado.
50. Bir, G.S., User's Guide to PreComp (Pre-Processor for Computing Composite Blade Properties). 2005, National Renewable Energy Laboratory: Golden, Colorado.